



*Research article*

## **JQ1 inhibits high glucose-induced migration of retinal microglial cells by regulating the PI3K/AKT signaling pathway**

**Ying Zhu<sup>1,†</sup>, Lipeng Guo<sup>2,†</sup>, Jixin Zou<sup>1</sup>, Liwen Wang<sup>1</sup>, He Dong<sup>1</sup>, Shengbo Yu<sup>3</sup>, Lijun Zhang<sup>1,\*</sup>, Jun Li<sup>4,\*</sup> and Xueling Qu<sup>5,\*</sup>**

<sup>1</sup> Department of Ophthalmology, Eye Hospital of Dalian, Dalian Third People's Hospital Affiliated of Dalian Medical University, Dalian 116037, China

<sup>2</sup> Department of Cardiovascular, Dalian Third People's Hospital Affiliated of Dalian Medical University, Dalian 116037, China

<sup>3</sup> Department of Anatomy, Dalian Medical University, Dalian 116044, China

<sup>4</sup> He Eye Specialists Hospital of ShenYang No. 128, Huanghebei Street, YuHong District, Shenyang 110034, China

<sup>5</sup> Pelvic Floor Repair Center, the Affiliated Dalian Maternity Hospital of Dalian Medical University, 1 Dunhuang Road, Dalian, China

† Ying Zhu and Lipeng Guo contributed equally to this work.

\* **Correspondence:** Email: [lijunzhangw@sina.com](mailto:lijunzhangw@sina.com), [robin\\_lijun@sina.com](mailto:robin_lijun@sina.com), [quxuelingmm@sina.com](mailto:quxuelingmm@sina.com).

**Abstract:** Diabetic retinopathy (DR) is one of the main leading causes of visual impairment worldwide. The current study elucidates the role of JQ1 in DR. A diabetic model was constructed by STZ injection and a high-fat diet. After establishment of the diabetic model, rats were assigned to treatment groups: 1) control, 2) diabetic model, and 3) diabetic+JQ1 model. *In vitro* Transwell and wound-healing assays were used to measure BV2 cell viability by stimulation with low glucose and high glucose with or without JQ1 and 740Y-P. Pathological methods were used to analyze DR, and Western blotting was used to analyze protein expression. Identification of enriched pathways in DR was performed by bioinformatics. Histopathological examination demonstrated that JQ1 rescued the loss of retinal cells and increased the thickness of retinal layers in diabetic rats. JQ1 attenuated high glucose-stimulated BV2 microglial motility and migration. The bioinformatics analysis implied that the PI3K-Akt signaling pathway was enriched in DR. JQ1 decreased the phosphorylation of PI3K and AKT as well as the immunostaining of PI3K in BV2 cells. 740Y-P (a PI3K agonist) significantly

reversed the decrease in p-PI3K and p-AK in BV2 cells. Additionally, JQ1 decreased the protein expression of p-PI3K, p-AKT, and MMP2/9 and immunostaining of PI3K in retinal tissues of rats. JQ1 suppresses the PI3K/Akt cascade by targeting MMP expression, thus decreasing the viability and invasion capacity of retinal microglia, suggesting an interesting treatment target for DR.

**Keywords:** JQ1; diabetic retinopathy; DR; PI3K/Akt; retinal microglia; RPs

---

## 1. Introduction

Diabetic retinopathy (DR) is a microvascular disorder resulting from diabetes that causes retinal ischemia, macular edema, and permanent loss of vision. The most prevalent microvascular complication of diabetes, DR, is a major contributor to visual impairment in adults between the ages of 24 and 75 [1,2]. Earlier studies have suggested that chronic hyperglycemia-induced new vessel formation and progressive retinal structure production contribute to the progression of DR [3,4]. At present, antihyperglycemia drugs, laser photocoagulation, and vitreoretinal surgery are the major treatments for DR [5,6]. However, further studies are needed to understand the molecular mechanisms involved in the progression of DR to block the progression of retinal neovascularization [7,8].

Microglia can be regarded as innate immune cells in the retina and play critical roles in retinal vascular angiogenesis and vasculopathy. The activation of microglial cells has already been found in diabetic retinas and is greatly involved in the regulation of DR development [9,10]. However, it is still unknown what molecular process causes DR to develop [11].

JQ1, a novel small-molecule bromodomain-containing protein (BRD) inhibitor, has been found to inhibit tumor growth and cell proliferation in many diseases. Qiu et al. indicated that JQ1 is an efficacious antitumor agent in ovarian cancer. Wang et al. [12] indicated that targeting c-Myc via JQ1 has an antitumorigenic effect on endometrial cancer. Meanwhile, JQ1 is a key regulator of autophagy that contributes to the inhibition of BC cell proliferation [13]. Moreover, Mu et al. indicated that JQ1 has a therapeutic effect on diabetic cardiomyopathy [14]. Wu et al. [15] indicated that JQ1 may improve diabetic atherosclerosis by preventing the proliferation and migration of VSMCs. Likewise, JQ1 treatment modulates Nox4-Nrf2 redox imbalance in the hippocampus and may be a promising agent for diabetes-associated cognitive dysfunction [16]. Although much evidence suggests a positive role for JQ1 in the treatment of diabetes and its complications, no article has systematically revealed the specific role JQ1 has played in the treatment of DR [17]. In this study, we provide an overview of the part played by BV2 microglial cells in initiating the emergence of DR during hyperglycemia and the amelioration of DR by JQ1.

## 2. Materials and methods

### 2.1. Experimental animals

Adult male Sprague–Dawley rats (6–8 weeks, weighing 220–250 g) were used. The diabetic model was constructed by injecting streptozotocin (STZ; 60 mg/kg in 50 mM citrate buffer, Sigma) intraperitoneally into rats and feeding them a high-fat diet (59% sucrose, 30% egg, 10% lard, and 1% cholesterol). After four weeks, the blood glucose concentrations of the rats were examined, and a blood

glucose level higher than 16.7 mmol/L was considered to indicate diabetes. Rats were randomly divided into a diabetic model group (DM,  $n = 6$ ), a normal control group (NC,  $n = 6$ ), and a diabetic+JQ1 model group (DM+JQ1,  $n = 6$ ). Additionally, the rats in the DM+JQ1 group were injected with JQ1 (50 mg/kg) intraperitoneally daily for one week. All animal protocols were conducted according to the guidance approved by the Institutional Animal Care and Use Committee of China Medical University.

## 2.2. BV2 microglia culture

Rat BV2 microglia were cultured in DMEM supplemented with 10% heat-inactivated fetal bovine serum (Gibco), 100 U/ml penicillin and 100  $\mu$ g/ml streptomycin (Invitrogen). After culturing for 12 h at 37 °C, the BV2 cells reached approximately 90% confluency, and they were randomly separated into three groups: the high glucose group, control group, and high glucose + JQ1 group. The cells in the high glucose group were transferred to high glucose medium (Invitrogen) for 24 h, and the cells in the high glucose + JQ1 group were further cultured in JQ1 for an additional 24 h.

## 2.3. Immunofluorescence

Retinal tissues and BV2 cells were prepared for immunofluorescence staining as previously described. Rats were slaughtered by intraperitoneal injection of ketamine/xylazine (10/2 mg/ml), and the eyes were removed after 1 hour of prefixing with 4 percent paraformaldehyde (PFA) at room temperature [18]. The anterior segments of the eyeball were then removed using a microscope (SMZ-168, Motic). The rest was fixed in 4% PFA overnight, dehydrated in 30% sucrose in PBS and then embedded at the optimal cutting temperature (Tissue Tek, Sakura, Japan). Then, 10-mm-thick sections were cut using a Leica microtome (Germany) and stored at -80 °C until use. For immunofluorescent staining, BV2 cells were plated in 24-well plates on glass coverslips and then fixed with 4% PFA. The slides were then incubated with 3% bovine serum albumin and permeabilized with 0.3% Triton X-100 (Beyotime, China) followed by incubation with primary antibodies at 37 °C for 1 hour. The tissue sections were incubated in PBS for 20 min and washed three times in PBS. Subsequently, the cells were incubated overnight at 4 °C with primary antibody. After washing three times with PBS, the sections were incubated with the appropriate secondary antibody for 2 hours. All antibodies were obtained from Abcam (Cambridge, USA), including p-PI3K antibody (1:50 dilution). Nuclei were counterstained with DAPI (Sigma–Aldrich). Images were examined under a fluorescence microscope (Dmi8, Leica, Germany).

## 2.4. Western blot analysis

Following homogenization, total protein was extracted for analysis from BV2 cells and retinal tissues. The tissue and cell homogenates were lysed using RIPA lysis buffer and centrifuged at 10,000 rpm for 20 min at 4 °C using a cooling centrifuge. The protein was loaded on a 10% SDS–PAGE gel and then transferred onto a polyvinylidene fluoride (PVDF) membrane (BioRad, Hercules, CA). The membranes were then blocked with 5% skimmed milk for 1 h and incubated with primary antibodies at 4 °C overnight. After incubation with conjugated secondary antibody for 1 h at room temperature, the protein bands were analyzed using image processing software.  $\beta$ -actin was used as a loading control.

All antibodies were obtained from Abcam (Cambridge, USA), including p-PI3K (1:1000 dilution), total PI3K (1:1000 dilution), p-AKT (1:1000 dilution), total AKT (1:1000 dilution), MMP-2 (1:1500 dilution), MMP-9 (1:2000 dilution), and  $\beta$ -actin (1:5000 dilution).

### 2.5. Transwell assay

BV2 cells ( $1 \times 10^5$  cells/well) were diluted with serum-free culture medium and transferred into the upper chamber of a 24-well Transwell insert system. Culture medium containing 5% FBS was added to the lower chamber. After 24 and 48 hours of incubation, the nonmigrating cells were gently removed with a cotton swab from the upper chamber. Cells that migrated through the lower side of the membrane were fixed with 4% paraformaldehyde and stained with a solution of 0.5% crystal violet (Beijing Solarbio Science & Technology Co., Ltd.) for 20 min. Photomicrographs of migrated cells were taken using an inverted optical microscope (Olympus CK2; Tokyo, Japan), and 5 random fields of view were selected to count the cell numbers.

### 2.6. Wound-healing assay

Cell migration was examined by wound-healing assay as previously described. In short, BV2 cells were cultured in 24-well plates. At near confluence, cells were grown in EBM-2 complete medium with 0.2% FBS for 3 h. A scratch was made with a sterile 200- $\mu$ l tip in each well after cell proliferation. Cell migration into the open wound was observed by microscopy. ImageJ was used to quantify the digital photographs of the migrated cells.

### 2.7. Histological staining

Retinal tissues were embedded in paraffin to prepare 4- $\mu$ m-thick sections. The sections were deparaffinized, hydrated with ethanol, and stained with hematoxylin and eosin. Each section was measured by a LEICA DM3000 microscope under 400 $\times$  magnification.

### 2.8. Microarray-based bioinformatics

Microarray analysis was performed to evaluate gene expression in DR, and the differentially expressed genes were studied using the GSE161533, GSE17351, GSE75241 and GSE67269 datasets downloaded from the GEO database. The differentially expressed genes were obtained with  $|\log_{2}FC| > 2$  and  $padj < 0.05$ . The “limma” package in R software was used to screen DEGs, and the “pheatmap” package was used to plot the heatmap. String was applied for pathway analysis to obtain gene-enriched items of biological processes. The DAVID online gene functional annotation tool (<https://david.ncifcrf.gov/>) was applied to evaluate the function and enriched pathways of candidate DEGs. The Fisher exact P value was applied as the enrichment degree. The enriched GO and KEGG pathway annotations for both up- and down-regulated DEGs were obtained.

### 2.9. Statistical analysis

Statistical analysis was carried out using SPSS 20.0 (Chicago, IL, USA). Data are presented as

the means  $\pm$  standard errors (SE). Student's t test was used to compare differences between two means. One-way analysis of variance (ANOVA) was used for multiple comparisons. Differences were considered statistically significant when the P value was 0.05 or less.

### 2.10. Ethics approval of research

This animal study was approved by the Ethics Committee of China Medical University (YL-OL-SD-65-2020-10) from ShenYang City, LiaoNing Province, China.

## 3. Results

### 3.1. The effect of JQ1 on diabetes-induced alterations in retinal layers

We examined the effect of JQ1 on diabetes-induced alterations in the ganglion cell layer (GCL). Hematoxylin-eosin staining was performed on retinal cryosections from experimental rats at 1, 3 and 7 days. Diabetic rats exhibited a significant decrease in the thickness of the GCL. Moreover, treatment with JQ1 recovered the decreased thickness of the GCL (Figure 1A). Similar decreases were seen in Figure 1B, and the total number of cells in the GCL was also diminished in the DM group at 3 and 7 days. The results showed that, compared with that in the DM group, the total number of cells in the GCL was restored in the JQ1 group at 3 and 7 days (Figure 1B,  $P < 0.05$ ). These results implied that JQ1 treatment can rescue the increased loss of retinal cells and the decreased thickness of retinal layers in diabetic rats.

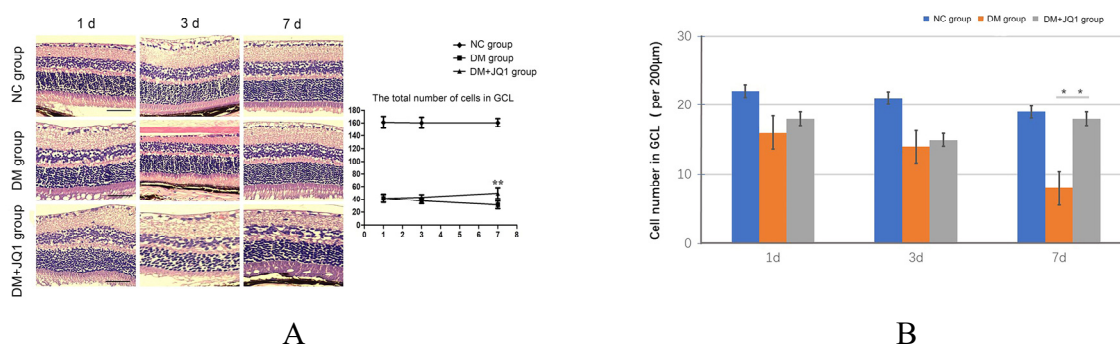


**Figure 1.** The effect of JQ1 on diabetes-induced alterations in the ganglion cell layer (GCL). A. Hematoxylin-eosin staining revealed that diabetic rats exhibited a significant decrease in the thickness of the GCL, and JQ1 reversed this decrease. B. The total number of cells in the GCL was decreased in the DM group compared with the JQ1 group at 3 and 7 days.  $P < 0.05$ . JQ1 group vs. DM group.

### 3.2. JQ1 attenuated high glucose-stimulated BV2 microglial motility

To assess the effect of JQ1 on BV2 microglial motility, we carried out a scratch wound assay. Representative images indicated that high glucose stimulation increased the migratory potential of the BV2 cells compared to the control at 12 and 24 h (Figure 2A). Treatment with JQ1 significantly

reduced BV2 cell motility in the coculture with high glucose medium in a time-dependent manner. Subsequently, it was demonstrated (Figure 2B) that the alteration in the width of the high glucose group was the most obvious compared with that of the control and high glucose + JQ1 groups at 12 and 24 hours after wounding ( $P < 0.05$ ). These results implied that JQ1 reduced high glucose-stimulated BV2 microglial motility.

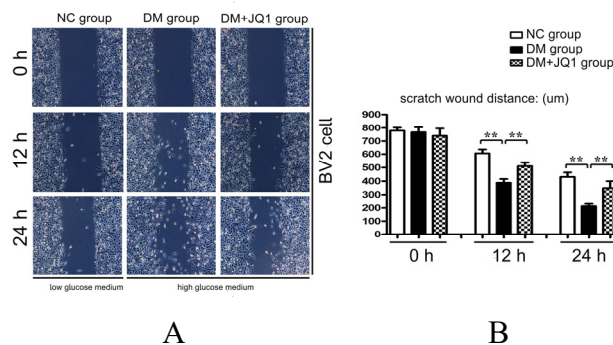


**Figure 2.** JQ1 inhibited microglial motility after 24 h. A. The scratch test revealed that BV2 microglial cell migration was markedly increased by high glucose stimulation at 24 and 48 h and was efficiently reduced by JQ1 transfection. B. Quantitative results of the scratch wound assay in BV2 cells,  $*P < 0.05$ , control, high glucose + JQ1 compared to the high glucose group. The results are the mean  $\pm$  standard deviation.

### 3.3. JQ1 inhibited the migration of BV2 cells

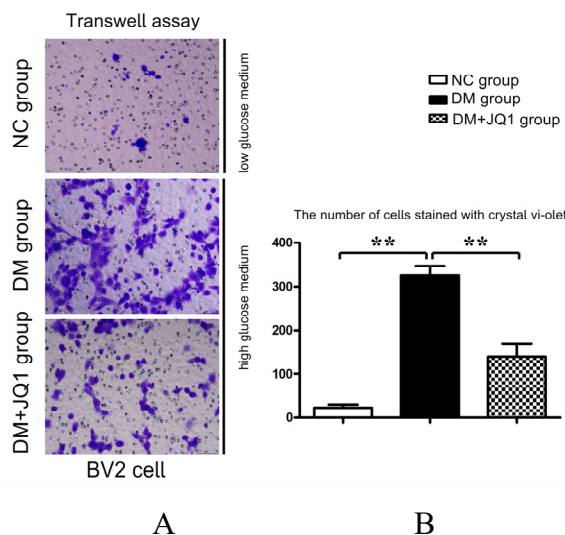
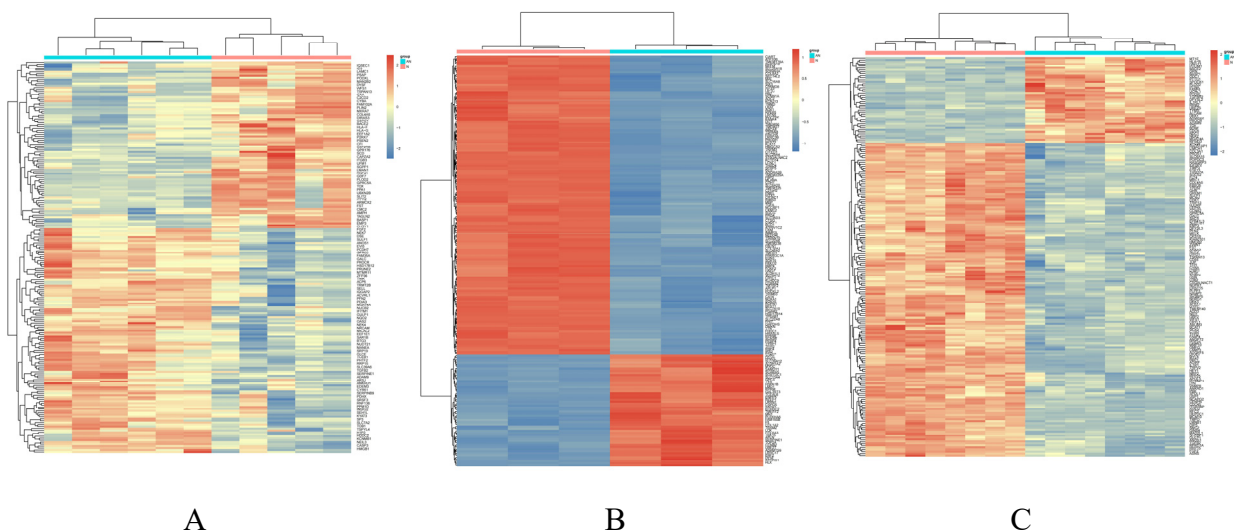


**Figure 3.** JQ1 inhibited the migration of BV2 cells. A. Transwell assays showed that BV2 microglial cell migration was markedly increased by high glucose stimulation and was effectively reduced by JQ1 transfection. B. Quantitative results of the Transwell assay in BV2 cells,  $P < 0.05$ , control, high glucose + JQ1 compared to the high glucose group. The results are the mean  $\pm$  standard deviation.

Transwell assays were carried out to further investigate the effect of JQ1 on the migration of BV2 cells. Similar to the scratch wound assay, the Transwell migration assay revealed that the migratory capacity of the BV2 cells was not altered in the control group (Figure 3A). We found that high glucose stimulation significantly enhanced the number of migrating BV2 cells. However, cotreatment with JQ1 and high glucose reduced the number of migrating BV2 cells. In addition, the outcomes of the experiment (Figure 3B) suggested that the number of cells stained with crystal violet in the high glucose group was greater than that in the control and high glucose + JQ1 groups ( $P < 0.05$ ). The Transwell assay illustrated that the migration of BV2 microglial cells was significantly improved after JQ1 treatment.

### 3.4. The PI3K-Akt signaling pathway was enriched in DR

The PI3K/Akt cascade is crucial in regulating a number of cellular processes, such as cell division, survival, and decomposition. [19,20] Here, we examined gene expression profiles and performed gene ontology (GO) and Kyoto Encyclopedia of Genes and Genomes (KEGG) classification analysis using data from the Gene Expression Omnibus (GEO) database, which contains diabetic retinopathy samples. We evaluated gene expression profiles from the GSE53257, GSE60436 and GSE70752 datasets. DEGs were determined in these datasets at a P value  $< 0.05$  and log fold change  $> 2$ . Heatmaps were depicted with the top 200 DEGs of the GSE53257 (Figure 4A), GSE60436 (Figure 4B) and GSE70752 datasets (Figure 4C). String was applied for pathway analysis to obtain gene-enriched items of biological processes. The results revealed that signal transduction, extracellular matrix organization, and cell adhesion were enriched pathways in DR from the GSE53257 and GSE70752 datasets (Figure 4D,E). The consistent visual charts of GO enrichment pathways for upregulated and downregulated differentially expressed genes from the data in the GSE60436 dataset are presented in Figure 4F,G, including extracellular matrix organization, cell migration and positive regulation of cell migration. Likewise, partial results of the KEGG pathways in the GSE60436 dataset are shown in Figure 4H, including the PI3K-Akt signaling pathway. These results implied that the PI3K-Akt signaling pathway was enriched in DR.



*Continued on next page*

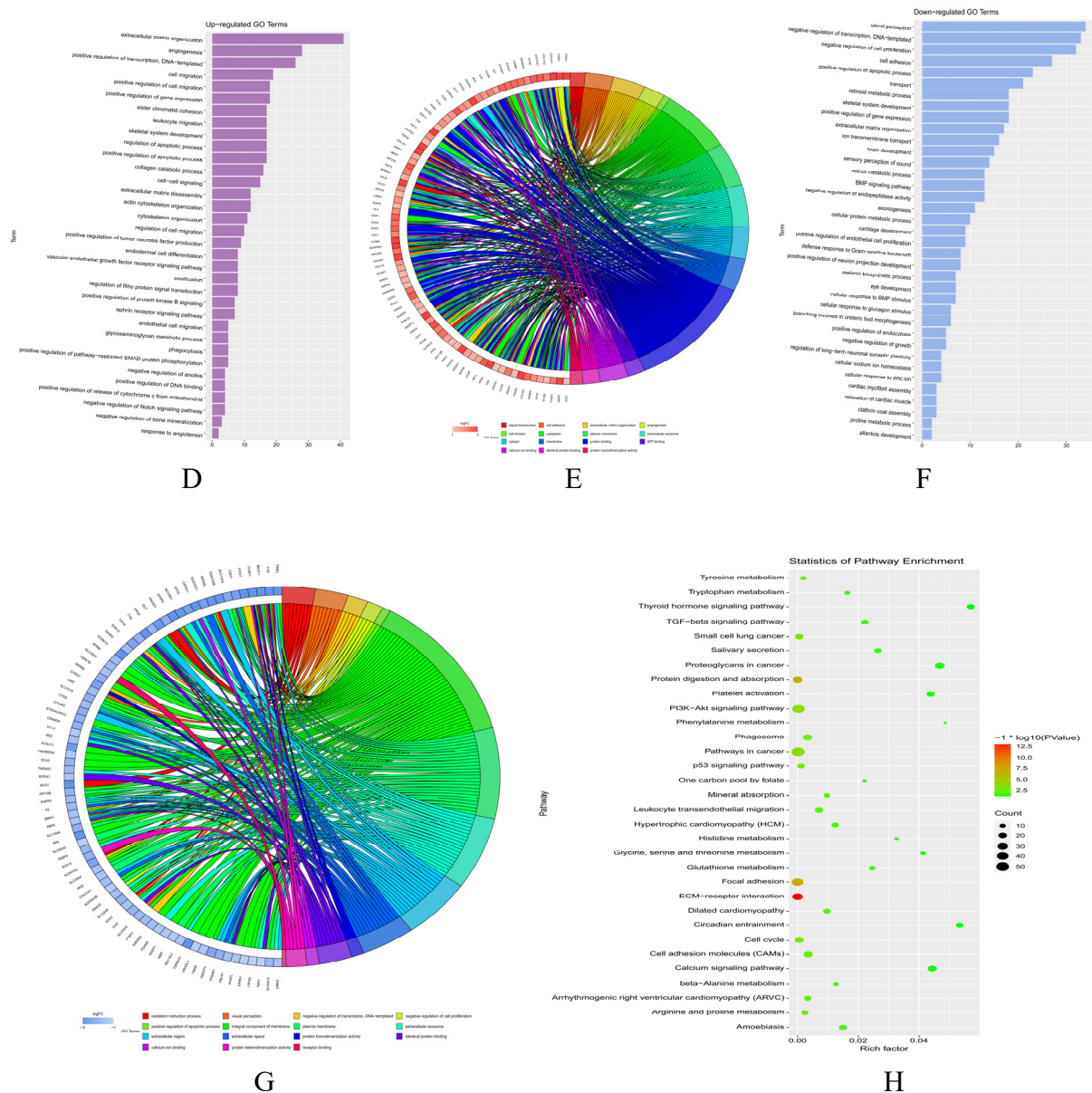


**Figure 4.** The PI3K-Akt signaling pathway was enriched in diabetic retinopathy. A–C. Diabetic retinopathy-related differentially expressed genes in the GSE53257, GSE60436 and GSE70752 datasets. The heatmap shows the differentially expressed genes. D–E. String was applied for pathway analysis to obtain gene-enriched items of biological processes from the GSE53257 and GSE70752 datasets. F–G. GO enrichment pathways for upregulated and downregulated differentially expressed genes from the GSE60436 dataset. H. Partial results of the KEGG pathways from the GSE60436 dataset.

### 3.5. JQ1 repressed BV2 microglial activation by inhibiting PI3K activation

Next, we focused on the effect of JQ1 on the PI3K/AKT pathway in retinal BV2 microglial cells. BV2 cells were cocultured with JQ1 and high glucose. Western blot analysis confirmed that high glucose stimulation enhanced the protein expression of p-PI3K and p-AKT in BV2 cells. However, the increase in p-PI3K and p-AKT protein expression was suppressed by JQ1. We discovered that



compared with the control and high glucose + JQ1 groups, the protein expression of p-PI3K and p-AKT in the BV2 cells in the high glucose group was significantly upregulated ( $P < 0.05$ ). Collectively, these results suggested that JQ1 specifically affected PI3K/AKT pathway activation in high glucose-stimulated BV2 microglial cells. To investigate whether PI3K was involved in regulating retinal BV2 cells, we examined the effects of 740Y-P, a PI3K agonist, in BV2 cells. The results indicated that 740Y-P significantly enhanced the protein expression of p-PI3K and p-AKT in high glucose + JQ1-stimulated retinal BV2 microglial cells (Figure 5). Furthermore, we verified PI3K activation in BV2 microglial cells. The level of p-PI3K was significantly increased in the high glucose group compared to that in the JQ1 and control groups, as shown by immunofluorescence staining and quantitative analysis. Based on these findings, JQ1 decreased PI3K activity and hence suppressed the activation of BV2 microglia in response to high glucose stimulation.

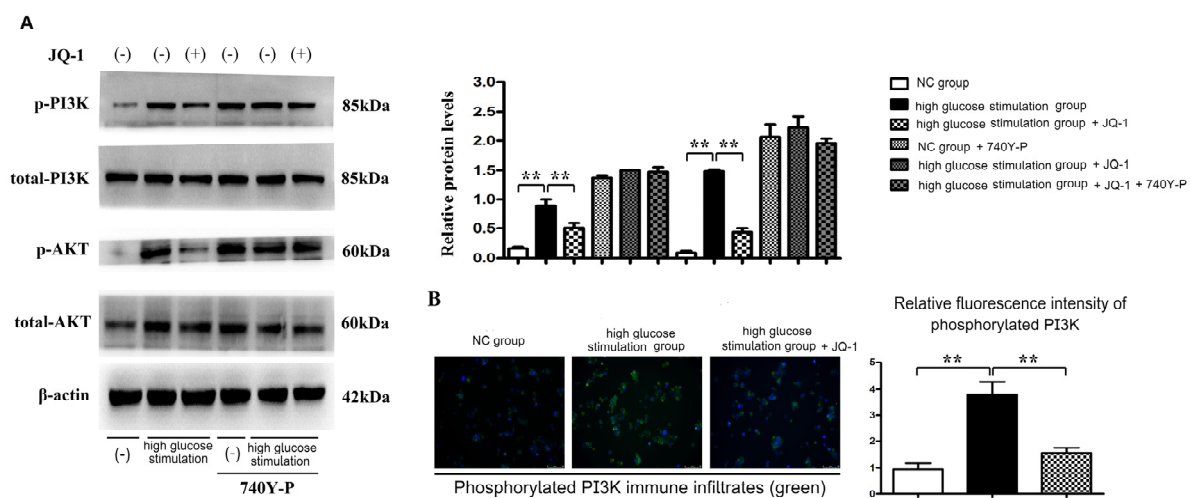
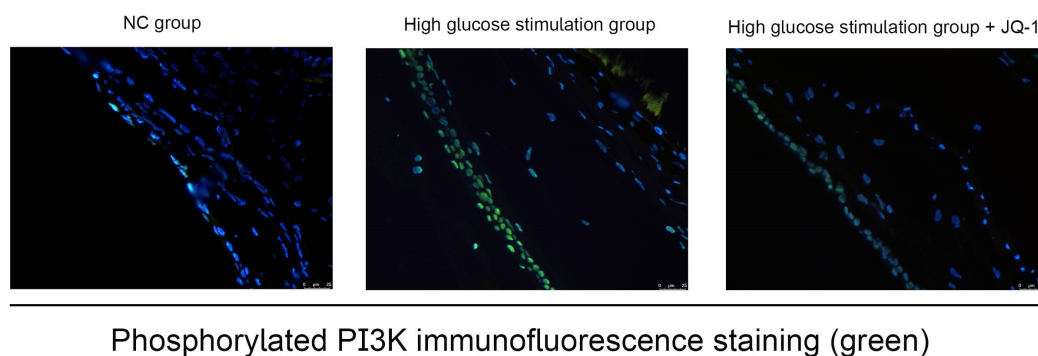


**Figure 5.** JQ1 repressed BV2 microglial activation by inhibiting PI3K activation. A. The relatively high protein expression levels of t-PI3K, t-AKT, p-PI3K and p-AKT observed in retinal BV2 cells before and after 740Y-P injection, as detected by western blot analysis.  $P < 0.05$ , high glucose, control group compared with the high glucose + JQ1 group. B. Immunofluorescence staining for p-PI3K in retinal BV2 cells.  $P < 0.05$ , high glucose, control group compared with the high glucose + JQ1 group.

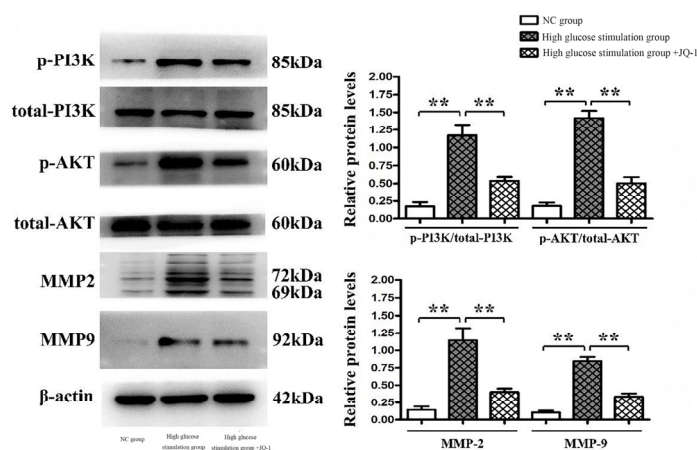
### 3.6. JQ1 decreased the expression of p-PI3K and MMP2/9 in diabetic retinopathy rats

In subsequent experiments, we attempted to detect the underlying mechanism for the protective effect of JQ1 in diabetic retinopathy *in vivo*. The immunofluorescence results showed a similar tendency to the *in vitro* results. As shown in Figure 6A, the expression of p-PI3K was increased in the retinal tissues of high glucose-stimulated rats. Treatment with JQ1 significantly reduced the expression of p-PI3K in the same sections of retinal tissues. In addition, Western blot analysis confirmed that treatment of rats with high glucose + JQ1 significantly decreased the protein expression of p-PI3K and p-AKT. Most importantly, our results showed that JQ1 suppressed the protein expression of MMP2 and MMP9 induced by high glucose stimulation in rats. The western blot results (Figure 6B) suggested

that the relative protein expression of p-PI3K, p-AKT, MMP2 and MMP9 was significantly increased in the retinal tissues of high glucose-stimulated rats, whereas the expression levels were significantly lower in retinal tissues of high glucose + JQ1 rats ( $P < 0.05$ ).



A



B

**Figure 6.** JQ1 decreased the expression of p-PI3K and MMP2/9 in diabetic retinopathy rats. A. Immunofluorescence staining in vivo. B. Western blot analysis for p-PI3K, p-AKT, MMP2 and MMP9.  $P < 0.05$ , high glucose, control group compared with the high glucose + JQ1 group.

#### 4. Discussion

DR is the most common complication of diabetes and a leading cause of vision loss worldwide. Retinal angiogenesis has been reported to be related to the pathogenesis of DR [21]. [22] Emerging evidence indicates that JQ1 suppresses tumor growth and cell proliferation [13,23], and PI3K was also reported to induce endothelial growth factor (VEGF) expression, which is an important contributor to DR development [24,25]. Therefore, exploring the involvement of JQ1 regulation may be an effective strategy to repress the progression of DR.

In the present study, we studied the impacts of JQ1 on diabetic retinopathy BV2 microglial cells and the role of JQ1 in the regulation of PI3K. The diabetic model was constructed by injecting STZ

intraperitoneally into rats and feeding them a high-fat diet. Hematoxylin-eosin staining showed that diabetic rats exhibited a significant decrease in the thickness of the GCL, whereas JQ1 treatment recovered the decreased thickness of the GCL. The total number of cells in the GCL showed the same trend; compared with that in the DM group, the number of cells in the GCL was increased in the JQ1 group. These results implied that JQ1 treatment rescued the increased loss of retinal cells and the decreased thickness of retinal layers in diabetic rats.

Microglial activation was previously found to play important roles in the development of DR. Therefore, it is important to investigate the mechanisms of microglial activation and to explore effective treatment in DR [25]. In this study, we attempted to examine the connection between JQ1 treatment and microglial activation in DR. According to the scratch wound assay, high glucose stimulation increased the migratory potential of BV2 cells in a time-dependent way, whereas JQ1 treatment significantly reduced the motility of BV2 cells, suggesting that JQ1 reduced high glucose-stimulated BV2 microglial motility. The Transwell migration assay, which is similar to the scratch wound assay, showed that high glucose stimulation considerably enhanced the number of migrating BV2 cells, but cotreatment with JQ1 and high glucose decreased the rise in migrating BV2 cells. These results illustrated that the migration of BV2 microglial cells was significantly improved after JQ1 treatment. The PI3K/Akt cascade plays important roles in coordinating a variety of cellular functions, including cell proliferation, survival and degradation. Here, we examined gene expression profiles in combination with GO and KEGG classification analysis from the GEO database, which contains diabetic retinopathy samples [26]. Heatmaps were depicted with the top 200 DEGs of the GSE53257, GSE60436 and GSE70752 datasets. String revealed that signal transduction, extracellular matrix organization, and cell adhesion were enriched pathways in DR from the GSE53257 and GSE70752 datasets. The GO enrichment pathways for upregulated and downregulated differentially expressed genes from the GSE60436 dataset revealed that extracellular matrix organization, cell migration and positive regulation of cell migration were enriched pathways in DR. Likewise, partial results of the KEGG pathways revealed that the PI3K-Akt signaling pathway was a highly enriched pathway in DR.

Next, we focused on the effect of JQ1 on the PI3K/AKT pathway in retinal BV2 microglial cells. BV2 cells were cocultured with JQ1 and high glucose. Western blot analysis confirmed that high glucose stimulation enhanced the protein expression of p-PI3K and p-AKT in BV2 cells, whereas JQ1 suppressed this increase, demonstrating that JQ1 specifically affected PI3K/AKT pathway activation in high glucose-stimulated BV2 microglial cells. To further investigate whether PI3K was involved in regulating retinal BV2 cells, we further examined the effects of 740Y-P, a PI3K agonist, in BV2 cells. The results indicated that 740Y-P significantly recovered the protein expression of p-PI3K and p-AKT downregulated by JQ1 in retinal BV2 microglial cells. Immunohistochemical staining revealed that the phosphorylation of PI3K was significantly increased in the high glucose group compared to the JQ1 group. Based on these results, JQ1 effectively inhibited PI3K activation and thus restricted BV2 microglial activation under high glucose stimulation.

The *in vivo* results of this experiment indicated that p-PI3K immunostaining was increased in the retinal tissues of high glucose-stimulated rats, whereas treatment with JQ1 could significantly reduce the expression of p-PI3K in the same section of retinal tissues. Western blot analysis confirmed that treatment of rats with high glucose + JQ1 significantly decreased the protein expression of p-PI3K and p-AKT. Furthermore, our results showed that JQ1 suppressed the protein expression of MMP2 and MMP9 induced by high glucose stimulation. These *in vivo* and *in vitro* results suggested that JQ1 might be a good marker to assess microglial activation in DR.

Together, our findings confirmed that JQ1 exerted antiangiogenic and antiproliferation effects during the progression of diabetic retinopathy by inhibiting the MMP2/9 pathway via upregulation of the PI3K/Akt signaling cascade. This study confirmed that JQ1 might be a promising biomarker in diabetic retinopathy.

## Acknowledgments

This study was supported by the National Natural Science Foundation of China (82171032) and the Natural Science Foundation of Liaoning Province (2020-MS-338).

## Conflict of interest

The authors declare there is no conflict of interest.

## References

1. S. Babapoor-Farrokhran, K. Jee, B. Puchner, S. J. Hassan, X. Xin, M. Rodrigues, et al., Angiopoietin-like 4 is a potent angiogenic factor and a novel therapeutic target for patients with proliferative diabetic retinopathy, *Proc. Natl. Acad. Sci.*, **112** (2015), 3030–3039. <https://doi.org/10.1073/pnas.1423765112>
2. Y. C. Chang, W. C. Wu, Dyslipidemia and diabetic retinopathy, *Rev. Diabetic Stud.*, **10** (2012), 121–132. <https://doi.org/10.1900/RDS.2013.10.121>
3. L. Chen, C. Y. Cheng, H. Choi, M. K. Ikram, C. Sabanayagam, G. S. Tan, et al., Plasma metabolomic profiling of diabetic retinopathy, *J. Am. Diabetes Assoc.*, **65** (2016), 1099–1108. <https://doi.org/10.2337/db15-0661>
4. F. Semeraro, F. Morescalchi, A. Cancarini, A. Russo, S. Rezzola, C. Costagliola, Diabetic retinopathy, a vascular and inflammatory disease: Therapeutic implications, *Diabetes Metab.*, **45** (2019), 517–527. <https://doi.org/10.1016/j.diabet.2019.04.002>
5. I. N. Mohamed, S. A. Soliman, A. Alhusban, S. Matragoon, B. A. Pillai, A. A. Elmarkaby, A. B. El-Remessy, Diabetes exacerbates retinal oxidative stress, inflammation, and microvascular degeneration in spontaneously hypertensive rats, *Mol. Vision*, **18** (2012), 1457–1466.
6. Z. Zhuang, H. Hu, S. Y. Tian, Z. J. Lu, T. Z. Zhang, Y. L. Bai, Down-regulation of microRNA-155 attenuates retinal neovascularization via the PI3K/Akt pathway, *Mol. Vision*, **21** (2015), 1173–1184.
7. B. Bahrami, M. Zhu, T. Hong, A. Chang, Diabetic macular oedema: pathophysiology, management challenges and treatment resistance, *Diabetologia*, **59** (2016), 1594–1608. <https://doi.org/10.1007/s00125-016-3974-8>
8. M. Henriksen, A. Nilsson, L. Janzon, L. Groop, The effect of glycaemic control and the introduction of insulin therapy on retinopathy in non-insulin-dependent diabetes mellitus, *Diabetic Med.*, **14** (1997), 123–131. [https://doi.org/10.1002/\(SICI\)1096-9136\(199702\)14:2<123::AID-DIA306>3.0.CO;2-U](https://doi.org/10.1002/(SICI)1096-9136(199702)14:2<123::AID-DIA306>3.0.CO;2-U)
9. J. Yin, W. Q. Xu, M. X. Ye, Y. Zhang, H. Y. Wang, J. Zhang, et al., Up-regulated basigin-2 in microglia induced by hypoxia promotes retinal angiogenesis, *J. Cell. Mol. Med.*, **7** (2017), 14925. <https://doi.org/10.1111/jcmm.13256>

10. E. Kermorvant-Duchemin, A. C. Pinel, S. Lavalette, D. Lenne, W. Raoul, B. Calippe, et al., Neonatal hyperglycemia inhibits angiogenesis and induces inflammation and neuronal degeneration in the retina, *PLoS ONE*, **8** (2013), e79545. <https://doi.org/10.1371/journal.pone.0079545>
11. X. Chen, H. Zhou, Y. Gong, S. Wei, M. Zhang, Early spatiotemporal characterization of microglial activation in the retinas of rats with streptozotocin-induced diabetes, *Graefe's Arch. Clin. Exp. Ophthalmol.*, **253** (2015), 519–525. <https://doi.org/10.1007/s00417-014-2727-y>
12. H. Qiu, A. L. Jackson, J. E. Kilgore, Y. Zhong, L. L. Y. Chan, P. A. Gehrig, et al., JQ1 suppresses tumor growth through downregulating LDHA in ovarian cancer, *Oncotarget*, **6** (2015), 6915. <https://doi.org/10.18632/oncotarget.3126>
13. H. Qiu, J. Li, L. H. Clark, A. L. Jackson, L. Zhang, H. Guo, et al., JQ1 suppresses tumor growth via PTEN/PI3K/AKT pathway in endometrial cancer, *Oncotarget*, **7** (2016), 66809–66821. <https://doi.org/10.18632/oncotarget.11631>
14. S. Bakshi, C. McKee, K. Walker, C. Brown, G. R. Chaudhry, Toxicity of JQ1 in neuronal derivatives of human umbilical cord mesenchymal stem cells, *Oncotarget*, **9** (2018), 33853–33864. <https://doi.org/10.18632/oncotarget.26127>
15. J. Mu, D. Zhang, Y. Tian, Z. Xie, M. H. Zou, et al., BRD4 inhibition by JQ1 prevents high-fat diet-induced diabetic cardiomyopathy by activating PINK1/Parkin-mediated mitophagy in vivo, *J. Mol. Cell. Cardiol.*, **149** (2020). <https://doi.org/10.1016/j.yjmcc.2020.09.003>
16. Y. Wu, M. Zhang, C. Xu, D. Chai, F. Peng, J. Lin, Anti-diabetic atherosclerosis by inhibiting high glucose-induced vascular smooth muscle cell proliferation via Pin1/BRD4 pathway, *Oxid. Med. Cell. Longevity*, **2020** (2020), 1–13. <https://doi.org/10.1155/2020/4196482>
17. E. Liang, M. Ma, L. Wang, X. Liu, J. Xu, M. Zhang, The BET/BRD inhibitor JQ1 attenuates diabetes-induced cognitive impairment in rats by targeting Nox4-Nrf2 redox imbalance, *Biochem. Biophys. Res. Commun.*, 2017, S0006291X17321976. <https://doi.org/10.1016/j.bbrc.2017.11.020>
18. J. M. Zhou, S. S. Gu, W. H. Mei, J. Zhou, Z. Z. Wang, W. Xiao, Ginkgolides and bilobalide protect BV2 microglia cells against OGD/reoxygenation injury by inhibiting TLR2/4 signaling pathways, *Cell Stress Chaperones*, **21** (2016), 1037–1053. <https://doi.org/10.1007/s12192-016-0728-y>
19. H. Shen, J. Zhang, Y. Zhang, Q. Feng, H. Wang, G. Li, et al., Knockdown of tripartite motif 59 (TRIM59) inhibits proliferation in cholangiocarcinoma via the PI3K/AKT/mTOR signalling pathway, *Gene*, **698** (2019), 50–60. <https://doi.org/10.1016/j.gene.2019.02.044>
20. Z. Y. Sun, Y. K. Jian, H. Y. Zhu, B. Li, lncRNAPVT1 targets miR-152 to enhance chemoresistance of osteosarcoma to gemcitabine through activating c-MET/PI3K/AKT pathway, *Pathol. Res. Pract.*, **215** (2019), 555–563. <https://doi.org/10.1016/j.prp.2018.12.013>
21. D. S. Boyer, J. J. Hopkins, J. Sorof, J. S. Ehrlich, Anti-vascular endothelial growth factor therapy for diabetic macular edema, *Ther. Adv. Endocrinol. Metab.*, **4** (2013), 151–169. <https://doi.org/10.1177/2042018813512360>
22. M. Ahmed, A. Asrar, Role of inflammation in the pathogenesis of diabetic retinopathy, *Middle East Afr. J. Ophthalmol.*, **19** (2012), 70. <https://doi.org/10.4103/0974-9233.92118>
23. T. Bagratuni, N. Mavrianou, N. G. Gavalas, K. Tzannis, C. Arapinis, M. Lontos, et al., JQ1 inhibits tumour growth in combination with cisplatin and suppresses JAK/STAT signalling pathway in ovarian cancer, *Eur. J. Cancer*, **126** (2020), 125–135. <https://doi.org/10.1016/j.ejca.2019.11.017>

24. X. Xu, Y. Zong, Y. Gao, X. Sun, H. Zhao, W. Luo, et al., VEGF induce vasculogenic mimicry of choroidal melanoma through the PI3k signal pathway, *BioMed Res. Int.*, **2019** (2019), 1–13. <https://doi.org/10.1155/2019/3909102>
25. N. Akeno, J. Robins, M. Zhang, M. F. Czyzyk-Krzeska, T. L. Clemens, Induction of vascular endothelial growth factor by IGF-I in osteoblast-like cells is mediated by the PI3K signaling pathway through the hypoxia-inducible factor-2alpha, *Endocrinology*, **143** (2002), 420–425. <https://doi.org/10.1210/endo.143.2.8639>
26. M. Jafari, E. Ghadami, T. Dadkhah, H. Akhavan-Niaki, PI3k/AKT signaling pathway: Erythropoiesis and beyond, *J. Cell. Physiol.*, **234** (2019), 2373–2385. <https://doi.org/10.1002/jcp.27262>



AIMS Press

©2022 the Author(s), licensee AIMS Press. This is an open access article distributed under the terms of the Creative Commons Attribution License (<http://creativecommons.org/licenses/by/4.0>)